JPET Fast Forward. Published on October 5, 2012 as DOI: 10.1124/jpet.112.198937

JPET #198937

Title

Differential cell-protective function of two resveratrol (trans-3,5,4'-trihydroxystilbene) glucosides against oxidative stress

Ryusuke Hosoda, Atsushi Kuno, Yusuke S. Hori, Katsuki Ohtani, Nobutaka Wakamiya, Azusa Oohiro, Hiroki Hamada, and Yoshiyuki Horio

Department of Pharmacology, School of Medicine, Sapporo Medical University (R.H., A.K, Y.S.H, Y.H.), Sapporo, 060-8556, Japan; Department of Microbiology and Immunochemistry, Asahikawa Medical University (K.O., N.W.), Asahikawa 078-8510, Japan; Department of Life Science, Faculty of Science, Okayama University of Science (A.O., H.H.), Okayama, 700-0005, Japan.

JPET Fast Forward. Published on October 5, 2012 as DOI: 10.1124/jpet.112.198937
This article has not been copyedited and formatted. The final version may differ from this version.

Running Title Page

Biological functions of glycosyl resveratrols

Address of corresponding author:
Yoshiyuki Horio, M.D., Ph.D.
Department of Pharmacology, School of Medicine, Sapporo Medical University, S1, W17, Chu-ouku, Sapporo 060-8556, Japan
Phone +81-11-611-2111 ex. 2720; fax +81-11-612-5861;
email: horio@sapmed.ac.jp

Number of Text pages: 31
Number of Tables: 2
Number of Figs: 7
Number of References: 30
Number of words in the Abstract: 247
Number of words in the Introduction: 354
Number of words in the Discussion: 937
Number of Supplemental Figs: 2

ABBREVIATIONS: AA, antimycin A; DPPH, 2, 2'-diphenyl-1-picrylhydrazyl; ESI-MS, electrospray ionization mass spectrometry; GAPDH, glyceraldehyde 3-phosphate dehydrogenase; GBA2, β-glucosidase 2; 3G-RSV, resveratrol-3-O-β-D-glucoside; 4'G-RSV, resveratrol-4'-O-β-D-glucoside; HPLC, high performance liquid chromatography; ORAC, oxygen radical absorbance capacity; PBS, phosphate buffered saline; PI, propidium iodide; ROS, reactive oxygen species; RSV, resveratrol; SGLT1, sodium-dependent glucose cotransporter 1; siRNA, small interfering RNA; SOD2, mitochondrial superoxide dismutase; TE, Trolox equivalent; Trolox, 6-hydroxy-2,5,7,8-tetramethylchroman-2-carboxylic acid; TUNEL, terminal deoxynucleotidyl transferase dUTP nick end-labeling.

Section assignment: Drug Discovery and Translational Medicine

JPET Fast Forward. Published on October 5, 2012 as DOI: 10.1124/jpet.112.198937
This article has not been copyedited and formatted. The final version may differ from this version.

ABSTRACT

Resveratrol (trans-3,5,4'-trihydroxystilbene, RSV), a natural polyphenol, exerts a beneficial effect on health and diseases. RSV targets and activates the NAD^+-dependent protein deacetylase SIRT1; in turn, SIRT1 induces an intracellular antioxidative mechanism by inducing mitochondrial superoxide dismutase (SOD2). Most RSV found in plants is glycosylated, and the effect of these glycosylated forms on SIRT1 has not been studied. Here, we compared the effects of RSV and two glycosyl RSVs, resveratrol-3-O-β-D-glucoside (3G-RSV, polydatin/piceid) and resveratrol-4'-O-β-D-glucoside (4'G-RSV), at the cellular level. In oxygen radical absorbance capacity (ORAC) and 2,2-diphenyl-1-picrylhydrazyl (DPPH) radical scavenging assays, 3G-RSV's antioxidant activity was comparable to that of RSV, while 4'G-RSV's radical-scavenging efficiency was less than 50% of that of RSV. However, 4'G-RSV, but not 3G-RSV, induced SIRT1-dependent histone H3 deacetylation and SOD2 expression in mouse C2C12 skeletal myoblasts; as with RSV, SIRT1 knockdown blunted these effects. RSV and 4'G-RSV, but not 3G-RSV, mitigated oxidative stress-induced cell death in C2C12 cells and primary neonatal rat cardiomyocytes. RSV and 4'G-RSV inhibited C2C12 cell proliferation, but

JPET Fast Forward. Published on October 5, 2012 as DOI: 10.1124/jpet.112.198937
This article has not been copyedited and formatted. The final version may differ from this version.

3G-RSV did not. RSV was found in both the intracellular and extracellular fractions of C2C12 cells that had been incubated with 4'G-RSV, indicating that 4'G-RSV was extracellularly deglycosylated to RSV, which was then taken up by the cells. C2C12 cells did not deglycosylate 3G-RSV. Our results point to 4'G-RSV as a useful RSV prodrug with high water solubility. These data also show that the *in vitro* antioxidative activity of these molecules did not correlated with their ability to protect cells from oxidative stress-induced apoptosis.

JPET Fast Forward. Published on October 5, 2012 as DOI: 10.1124/jpet.112.198937
This article has not been copyedited and formatted. The final version may differ from this version.

Introduction

Resveratrol (RSV), a defense antioxidant molecule found in plants, has various target molecules in mammalian cells. Its health benefits include activity against cancer (Jang et al., 1997), metabolic disease (Baur et al., 2006; Lagouge et al., 2006), diabetes (Su et al., 2006), atherosclerosis (Wu and Hsieh, 2011), and muscular dystrophy (Hori et al., 2011), as well as cardioprotective (Tanno et al., 2010), neuroprotective (Sun et al., 2010) effects. RSV targets and activates the NAD^+-dependent protein deacetylase SIRT1 (Howitz et al., 2003). RSV not only acts as an antioxidant itself, but also induces other intracellular antioxidative activity. We previously found that RSV decreases intracellular reactive oxygen species (ROS) levels by inducing SOD2 via SIRT1 activation in C2C12 myoblast cells and cardiomyocytes (Tanno et al., 2010), and that long-term RSV treatment decreases ROS levels and significantly prolongs survival in cardiomyopathic TO2 hamsters (Tanno et al., 2010).

Plants produce various RSV derivatives, among which glycosyl RSVs, especially resveratrol-3-O-β-D-glucoside (3G-RSV/polydatin/piceid), are prominent (Romero-Perez et al., 1999). Since 3G-RSV resists oxidation by tyrosinases, its half-life may be longer than that of RSV *in vivo* (Regev-Shoshani

et al., 2003). Glycosylation increases polyphenols' water solubility (Vogt and Jones, 2000), allowing for more convenient, efficient administration either orally or parenterally. We recently synthesized 3G-RSV and 4'-O-β-D-glucoside RSV (4'G-RSV) (Weis et al., 2006) from RSV using a glucosyltransferase expressed in *Escherichia coli* (Ozaki et al., 2012). Although unmodified RSV and 3G-RSV have the same antioxidative capacity *in vitro* (Fabris et al., 2008), the characteristics of 4'G-RSV have not been determined. Likewise, it has not been determined whether glycosyl RSVs can activate SIRT1 or exert other biological functions in cultured cells.

We found that resveratrol inhibits oxidative stress-induced cell death of C2C12 cells and cardiomyocytes (Tanno et al., 2010). In the present study, we used these cells to examine the properties of 3G-RSV and 4'G-RSV purified from cultured *Phytolacca Americana* plant cells. While RSV and 4'G-RSV exerted similar effects on myoblasts and cardiomyocytes, 3G-RSV had little or no effect on cellular function. We show here that while glycosyl RSVs are not transported into C2C12 cells, C2C12 cells can extracellularly deglycosylate 4'G-RSV to RSV, which then enters the cell.

JPET Fast Forward. Published on October 5, 2012 as DOI: 10.1124/jpet.112.198937
This article has not been copyedited and formatted. The final version may differ from this version.

Materials and Methods

Materials. RSV and Hoechst 33342 were purchased from Wako Pure Chemicals (Osaka, Japan). We synthesized 3G-RSV and 4'G-RSV (Fig. 1A) using RSV and *Phytolacca Americana* plant cells; 3G-RSV and 4'G-RSV were purified as previously reported (Ozaki et al., 2012). The purity of RSV, 3G-RSV, and 4'G-RSV used in the experiments was confirmed by high-performance liquid chromatography (HPLC) and electrospray ionization mass spectrometry (ESI-MS) (Supplemental Fig. 1). We used the following antibodies: rabbit polyclonal anti-acetyl-histone H3 (Calbiochem, San Diego, CA), rabbit polyclonal histone H3 (Abcam, Cambridge, MA), rabbit polyclonal anti-SOD2 (Millipore, Billerica, MA), rabbit polyclonal anti-SIRT1 (Sakamoto et al., 2004), mouse monoclonal anti-GAPDH, mouse monoclonal anti-α-tubulin (Sigma-Aldrich, St. Louis, MO), and rabbit anti-active caspase-3 antibody (ab32042, 1:200 dilution) (Abcam, Cambridge, MA). Other reagents were purchased from Wako Pure Chemicals or Sigma-Aldrich.

Oxygen radical absorbance capacity (ORAC) assay.

ORAC assay was based on the previous report by Prior et al. (Prior et al. 2003). Test samples were dissolved in 99.5% ethanol. The assay was carried out on a

Powerscan HT plate reader (DS Pharma Biomedical, Osaka, Japan). AAPH (2, 2'-azobis (2-amidinopropane) dihydrochloride) was used as peroxyl generator and Trolox (6-hydroxy-2,5,7,8-tetramethylchroman-2-carboxylic acid) as a standard. Trolox standard solution (6.25, 12.5, 25, and 50 μM) or blank, fluorescein solution and AAPH solution were incubated in assay buffer at 37°C in a 96-well plate. The fluorescence (Ex. 485 nm, Em. 530 nm) was monitored every 2 min for 90 min. The net AUC (area under the curve) were calculated by subtracting the AUC for blank from that for the sample or standard. The ORAC values were calculated from the Trolox standard curve. The ORAC value was expressed as micromoles of Trolox equivalent (TE) per micromole of sample.

DPPH (2,2-diphenyl-1-picrylhydrazyl) radical-scavenging activity. The DPPH radical-scavenging activity was measured as reported by Morales and Jiménez-Pérez (Morales and Jimenez-Perez, 2001), with a slight modification. Test samples in 500 μL of water were mixed with 500 μL of 99.5% ethanol containing 0.15 mM DPPH. This mixture was shaken and kept at room temperature for 30 min, and the absorbance of the mixture was measured at 517 nm. The results were calculated as percent inhibition according to the formula

JPET Fast Forward. Published on October 5, 2012 as DOI: 10.1124/jpet.112.198937
This article has not been copyedited and formatted. The final version may differ from this version.

[(C –SB) – (S – SB))/(C – SB)] x 100, where S, SB, and C are the absorbance of the sample, blank sample, and control, respectively.

Cell culture and treatment. C2C12 myoblast cells were cultured with Dulbecco's modified Eagle's medium (Wako Pure Chemical) supplemented with 1% antibiotic-antimycotic mixed stock solution (Nacalai Tesque, Kyoto, Japan) and 10% fetal bovine serum (MP Biomedicals, Solon, OH). Cells were seeded on glass slides for immunocytochemical studies. To examine histone deacetylation, C2C12 cells were pretreated for 18 h with 10 nM trichostatin A, which inhibits class I and II histone deacetylases, and then incubated with vehicle (dimethyl sulfoxide) or 100 μM RSV, 3G-RSV, or 4'G-RSV for 24 h. Cell samples were then analyzed by immunoblotting. SOD2 induction was examined by treating cells with vehicle or with 100 μM RSV, 3G-RSV, or 4'G-RSV for 24 h; 100 μM antimycin A (AA) was added 6 h before harvest to induce oxidative stress. Cell lysates were analyzed by immunoblotting, immunostaining, or quantitative RT-PCR.

Immunoblot analysis. Cells were lysed with CelLytic M Cell Lysis Reagent (Sigma-Aldrich) with 1% protease inhibitor cocktail (Nacalai Tesque), and centrifuged at 10,000 g for 10 min at 4 °C. The supernatant protein concentration

was measured with the Protein Quantification Kit-Rapid (Dojindo, Kumamoto, Japan). Equal protein amounts per lane (20 μg) were analyzed by immunoblotting as described previously (Hori et al., 2011), using the following antibodies: anti-acetyl-histone H3 (1:4000), anti-histone H3 (1:50000), anti-SOD2 (1:1000), anti-GAPDH (1:10000), and anti-α-tubulin (1:10000).

Immunostaining. Samples were fixed with 4% paraformaldehyde and treated for 30 min with phosphate buffered saline (PBS) containing 3% bovine serum albumin, 1% goat serum, and 0.1% Triton X-100. Next, samples were incubated with antibodies against SOD2 (1:1000 dilution) overnight at 4 °C, washed with PBS, incubated with secondary antibodies (1:2000 dilution) for 4 h at room temperature, and washed again with PBS. Samples were then incubated with Hoechst 33342 (1:1000 dilution) to stain the nucleus, and were mounted with VECTASHIELD (Vector Laboratories, Burlingame, CA). SOD2 levels were compared by image fluorescence intensity, quantified with Image J Software (National Institutes of Health, Bethesda, MD); 24 independent fields were examined in each experiment, and the data from three independent experiments were compared. To stain activated caspase-3, C2C12 cells were treated with 30 μM RSV, 3G-RSV, or 4'G-RSV for 4 h, and then cells were further incubated

JPET Fast Forward. Published on October 5, 2012 as DOI: 10.1124/jpet.112.198937
This article has not been copyedited and formatted. The final version may differ from this version.

with 50 μM antimycin A (AA) for 8 h in the absence of serum. Fixed cells were stained with anti-active caspase-3 antibody and Hoechst 33342. Five fields for each treatment were examined and the data from four independent experiments were compared.

Quantitative RT-PCR. Total RNA was isolated using the RNeasy Mini Kit (Qiagen, Valencia, CA). First-strand cDNA was synthesized using SuperScript III (Invitrogen, Carlsbad, CA). DNA was amplified with TaqMan Universal Master Mix II with UNG (Applied Biosystems, Foster City, CA) and TaqMan Gene Expression Assays for SOD2 (Mm00449726_m1) or GAPDH (Mm99999915_g1). Data from three independent experiments were compared.

SIRT1 knockdown. Small interfering RNAs (siRNAs) for SIRT1 (SASI_Mm01_00105675) and control-siRNAs from Sigma Genosys were used as described previously (Hori et al., 2011). We used a Nucleofector kit (Lonza, Basel, Switzerland) to electroporate siRNA (100 nM) into C2C12 cells twice, 24 h apart, and the cells were used in experiments 24 h after the second electroporation.

Apoptosis assays in neonatal rat cardiomyocytes. Neonatal rat cardiomyocytes were isolated as previously reported (Tanno et al., 2010).

JPET Fast Forward. Published on October 5, 2012 as DOI: 10.1124/jpet.112.198937
This article has not been copyedited and formatted. The final version may differ from this version.

Propidium iodide (PI) staining was used to identify dead cells before pharmacological modulation, and PI^+-cells were eliminated for statistical analysis. Beginning 36 h after isolation, cells were incubated with vehicle or 40 μM RSV, 3G-RSV, or 4'G-RSV for 36 h; 100 μM antimycin A (AA) was added 24 h before harvest. Apoptotic cells were detected by TUNEL staining and nuclear condensation as previously described (Tanno et al., 2010). Six independent experiments were carried out and cells of 14 visual fields were counted in each experiment except for one experiment in which number of cells from seven visual fields was examined.

Cell-growth inhibition. C2C12 cells were treated with vehicle or 30 μM RSV, 3G-RSV, or 4'G-RSV for 24 h. Cells were fixed with 4% paraformaldehyde, stained by Hoechst 33342, and counted. Data from six independent experiments were compared.

Mass spectrometry and high-performance liquid chromatography. ESI-MS was performed with a JMS-LCmate (JEOL, Tokyo, Japan) in positive ionization mode (ESI+) with a methanol carrier solution at a 0.5 mL/min flow-rate and injection volume of 2 μl.

HPLC was performed with an MD-1510 and a reverse phase CRESTPAK

JPET Fast Forward. Published on October 5, 2012 as DOI: 10.1124/jpet.112.198937
This article has not been copyedited and formatted. The final version may differ from this version.

C18S column (150 × 4.6 mm) (Jasco, Tokyo, Japan). Data were analyzed by DP-L1500W (Jasco). The mobile phase consisted of acetonitrile and H_2O in a 15:85 ratio (v/v). The mobile phase was filtered through a 0.2-μm membrane and degassed by aspirator before analysis. A 20-μl sample was separated by the column at a 1.0 ml/min flow rate, and RSV and glycosyl RSVs were monitored at 323 nm. All experiments were performed at ambient temperature.

Intracellular and extracellular RSV and glycosyl RSV measurement. C2C12 cells cultured in a 10-cm dish were incubated with 100 μM RSV, 3G-RSV, or 4'G-RSV for 12 h, after which 10 ml of culture medium was transferred to a tube containing 10 ml of methanol. The mixture was shaken vigorously for 30 min at room temperature, and the methanol layer, which contained the RSV or RSV derivatives, was isolated and evaporated; dried samples were stored at -80 °C until use. After removing the culture medium, the cells were washed twice with PBS and lysed with CelLytic M Cell Lysis Reagent. The cell lysates were sonicated and centrifuged. The RSV and RSV derivatives were extracted from the supernatant fractions with equal volumes of methanol, and were dried. The samples were dissolved in 100 μl of methanol and examined by ESI-MS and HPLC in at least three independent experiments.

Statistical analysis. Results are presented as means ± S.E.M. All statistical analyses were carried out using SigmaStat (Systat Software, Chicago, IL). Differences were tested by a one-way ANOVA. A P value of <0.05 was considered significant.

JPET Fast Forward. Published on October 5, 2012 as DOI: 10.1124/jpet.112.198937
This article has not been copyedited and formatted. The final version may differ from this version.

Results

3G-RSV and 4'G-RSV antioxidative activity *in vitro*. We compared the *in vitro* antioxidative activity of 3G-RSV and 4'G-RSV with that of RSV, and found that while RSV and 3G-RSV had similar ORAC values, those of 4'G-RSV were much lower (Table 1). The DPPH-scavenging capacity was almost the same for 3G-RSV and RSV, whereas 4'G-RSV's capacity was about half that of RSV (Fig. 1B). The DPPH-scavenging half-maximal (50%) inhibitory concentration (IC50) of RSV and 3G-RSV was about 80 μM and 110 μM, respectively; however, 250 μM 4'G-RSV was needed to neutralize 50% of DPPH radicals. Thus, 3G-RSV's *in vitro* anti-oxidant activity was comparable to that of RSV, while 4'G-RSV was less able to eliminate ROS.

SIRT1-dependent induction of histone H3 deacetylation and SOD2 expression by 4'G-RSV. RSV promotes histone H3 deacetylation and increases SOD2 expression in a SIRT1-dependent manner (Tanno et al., 2010). The acetyl histone H3 level decreased significantly in C2C12 cells treated with RSV or 4'G-RSV, but were unaffected by 3G-RSV (Fig. 2A). In addition, the SOD2 mRNA level increased in C2C12 cells treated with RSV or 4'G-RSV, but not in those treated with 3G-RSV (Fig. 2B); immunostaining and immunoblotting

JPET Fast Forward. Published on October 5, 2012 as DOI: 10.1124/jpet.112.198937
This article has not been copyedited and formatted. The final version may differ from this version.

experiments showed the same to be true for SOD2 protein levels (Fig. 2, C and D).

We next tested whether 4'G-RSV exerted these effects by activating SIRT1. The SIRT1 protein level of C2C12 cells treated with SIRT1-siRNA was 38% of that in the cells treated with control-siRNA (Fig. 3A). RSV or 4'G-RSV promoted histone H3 deacetylation in cells transfected with control-siRNA, but not in SIRT1-knockdown cells (Fig. 3B). Knocking down SIRT1 also blunted the SOD2 protein increase induced by RSV or 4'G-RSV (Fig. 3C). Again, 3G-RSV treatment did not affect the SOD2 levels in cells transfected with either control-siRNA or SIRT1-siRNA (Fig. 3C).

4'G-RSV anti-apoptotic and anti-proliferative activity. We next examined the anti-apoptotic activity of the RSV derivatives. RSV inhibits oxidative stress-induced cell death in neonatal rat ventricular cardiomyocytes by activating SIRT1 (Tanno et al., 2010). Treatment with antimycin A (AA), which increases and releases ROS from mitochondria by inhibiting mitochondrial respiratory chain complex III, increased the number of C2C12 cells with condensed nuclei (Fig. 4A) and activated caspase-3 positive cells (Fig. 4B). Pretreating the cells with RSV or 4'G-RSV, but not 3G-RSV, significantly suppressed this increase

JPET Fast Forward. Published on October 5, 2012 as DOI: 10.1124/jpet.112.198937
This article has not been copyedited and formatted. The final version may differ from this version.

(Fig. 4, A and B). We also examined apoptosis of neonatal rat ventricular cardiomyocytes by TUNEL staining (Fig. 4C). AA increased the number of TUNEL-positive apoptotic cells, and that pretreatment with RSV or 4'G-RSV significantly suppressed this increase (Fig. 4C).

Since RSV arrests cell growth in some cells (Chen et al., 2010), we evaluated the effect of the glycosyl RSVs on cell growth by counting C2C12 cells after 24 h of treatment with 30 μM RSV, 3G-RSV, or 4'G-RSV (Fig. 5). RSV significantly inhibited the C2C12 cell proliferation; the RSV-treated cell population was less than 50% of that of the control cells. The cell proliferation was moderately inhibited by 4'G-RSV; the 4'G-RSV-treated cell population was 73% of that of the control cells. Cell growth was not inhibited by 3G-RSV (Fig. 5).

Conversion of 4'G-RSV to RSV by C2C12 cells. Since these findings raised the possibility that 3G-RSV cannot permeate the C2C12 and cardiomyocyte cellular membranes, we next examined the cellular uptake of the glycosyl RSVs. C2C12 cells were treated with RSV, 3G-RSV, or 4'G-RSV for 12 h, washed twice with PBS, and lysed, after which RSV or RSV derivatives were extracted from the cell lysates and analyzed by ESI-MS (Fig. 6, A-C). RSV was found in the intracellular fraction of RSV-treated cells (Fig. 6A). However, 3G-RSV could not

JPET Fast Forward. Published on October 5, 2012 as DOI: 10.1124/jpet.112.198937
This article has not been copyedited and formatted. The final version may differ from this version.

be detected in the 3G-RSV-treated cells (Fig. 6B); thus, 3G-RSV poorly permeates the C2C12 cellular membrane. Interestingly, the intracellular fraction from 4'G-RSV-treated cells contained RSV but not 4'G-RSV (Fig. 6C). This raised the question of whether 4'G-RSV was transported into the cell and then deglycosylated into RSV, or whether the 4'G-RSV was extracellularly deglycosylated and the resultant RSV taken up by the cell.

To address this question, C2C12 cells were incubated with culture medium and 100 μM RSV, 3G-RSV, or 4'G-RSV for 12 h, and then cells and the culture medium were analyzed by an octa decyl silyl column. RSV, 3G-RSV, and 4'G-RSV are separated and identified with HPLC (Fig. 7) as shown by Ozaki et al. (Ozaki et al., 2012) and the contents of RSV or RSV derivatives were shown (Table 2). Both the cell fraction and the culture medium of RSV-treated cells contained RSV (Fig. 7, RSV and Table 2). Neither 3G-RSV nor RSV was detected in the cellular fraction of 3G-RSV-treated cells, although 3G-RSV was detected in the culture medium (Fig. 7, 3G-RSV and Table 2). Only RSV was detected in the intracellular fraction of 4'G-RSV-treated cells, although both 4'G-RSV and RSV were found in the culture medium (Fig. 7, 4'G-RSV and Table 2). When 4'G-RSV was incubated with culture medium in the absence of cells,

however, RSV was not detected in the culture medium, indicating that 4'G-RSV was deglycosylated by the C2C12 cells (Supplemental Fig. 2). Our results suggest that C2C12 cells metabolized 4'G-RSV extracellularly and took in the resulting RSV.

Discussion

While glycosylating RSV should increase its bioavailability by increasing its water solubility and stability, it has not been clear whether glycosyl RSV derivatives can retain the biological activity of unmodified RSV. In this study, we found that the *in vitro* antioxidant activity of 3G-RSV was comparable to that of RSV, while 4'G-RSV's antioxidant activity was less than 50% of that of RSV. However, treating cells with 4'G-RSV, but not 3G-RSV, induced histone deacetylation and SOD2 expression to the same degree as with RSV. We also found that 4'G-RSV, but not 3G-RSV, suppressed apoptosis and inhibited cell proliferation. These data clearly indicate that RSV derivatives do not necessarily exert the same cellular effects as native RSV, and that a compound's *in vitro* antioxidative activity does not necessarily reflect its ROS-scavenging capacity *in vivo*. In addition, the RSV glycosylation site is critical for a glycosyl RSV's antioxidative function.

RSV cellular uptake occurs by passive diffusion without the participation of transporters or pumps in human intestinal Caco-2 cells (Henry et al., 2005) and in the rat intestinal perfusion model (Juan et al., 2010). We found that neither 3G-RSV nor 4'G-RSV could enter C2C12 cells (Figs. 6 and 7). The enhanced

JPET Fast Forward. Published on October 5, 2012 as DOI: 10.1124/jpet.112.198937
This article has not been copyedited and formatted. The final version may differ from this version.

hydrophilic property of glycosyl RSVs compared to unmodified RSV may interfere with their diffusion across the lipid bilayer. As mentioned above, 3G-RSV offered little or no protection against oxidative stress (Fig. 4, A-C), indicating that reducing the extracellular ROS is not sufficient to protect cells; RSV must enter the cells to improve cell survival, at least under the conditions we used. Although Caco-2 cells are able to take up 3G-RSV slowly, the accumulation rate is only 25% that of RSV (Henry et al., 2005). Pharmacological examination suggested that 3G-RSV is transported by the sodium-dependent glucose cotransporter 1 (SGLT1) (Henry et al., 2005) that participates in glucose uptake in the brush-border membrane of the intestinal mucosa and the proximal tubule of the nephron (Wright et al., 2011). Wang et al. showed that 3G-RSV, administered intravenously, decreases the mitochondrial membrane potential and ATP level and inhibits mitochondrial swelling more effectively than RSV in arterial smooth muscle cells of a rat hemorrhage shock model (Wang et al., 2012). These results indicate that 3G-RSV and RSV differ in biological function *in vivo*. Although SGLT1 is ubiquitously expressed in various tissues including heart (Wright et al., 2011), neonatal rat cardiomyocytes and C2C12 cells were insensitive to 3G-RSV in our experiments, and C2C12 cells could not take up

3G-RSV. The reason for this discrepancy is not known.

We found that C2C12 cells could metabolize 4'G-RSV, but not 3G-RSV, into RSV. Although β-glucosidase from almonds is reported to metabolize 3G-RSV to RSV (Krasnow and Murphy, 2004), our experiment indicated that 4'G-RSV, but not 3G-RSV, was a substrate for β-glucosidase in C2C12 cells. Since 4'G-RSV effectively protected rat neonatal cardiomyocytes against oxidative stress (Fig. 4C), cardiomyocytes may express a β-glucosidase similar to that in C2C12 cells. The mammalian β-glucosidase family consists of four members: cytosolic β-glucosidase (de Graaf et al., 2001), the lactase expressed in the intestinal brush border membrane (Mantei et al., 1988), lysosomal β-glucosidase (β-glucocerebrosidase), which can cause Gaucher's disease if defective (Kacher et al., 2008), and membrane-bound β-glucosidase. Among these, membrane-bound β-glucosidase, also known as β-glucosidase 2 (GBA2) or non-lysosomal glucosylceramidase, is expressed in the widest variety of tissues, including heart and skeletal muscles, and has the widest substrate specificity (Matern et al., 2001). Deglycosylated products are found in the culture medium of cells expressing GBA2 when substrate is added extracellularly (Boot et al., 2007). These results suggest that GBA2 is an exoplasmic glucosidase and that it

JPET Fast Forward. Published on October 5, 2012 as DOI: 10.1124/jpet.112.198937
This article has not been copyedited and formatted. The final version may differ from this version.

catabolizes 4'G-RSV to RSV.

We found that the amount of intracellular RSV after incubation of C2C12 cells with 100 μM RSV was 5.34 ± 0.14 nmoles (Table 2). Because initial amount of RSV added to the culture medium was 1 μmoles, only 0.5% of RSV was detected in the cells (Table 2). Accordingly, resulting culture medium after incubation with RSV for 12 h contained unexpectedly low level of RSV and only 1.7% of RSV was recovered from the culture medium (Table 2). Sodium bicarbonate in the culture medium is reported to degrade RSV and 96% of RSV at a concentration of 200 μM is degraded in Base Modified Eagle Medium after 24 h incubation (Yang et al., 2010). Thus, extremely low levels of RSV and glycosyl RSVs in the culture medium and cells may be due to their degradation by the culture medium.

Whether SIRT1 is directly or indirectly activated by RSV is under debate (for a review see Horio et al., 2011). As SIRT1 activation by RSV derivatives may provide clues to help resolve this debate, we also intended to examine whether glycosyl RSVs activated SIRT1 in the present study. However, the glycosyl RSVs failed to enter cells. We tried to determine the glycosyl RSVs' effects on histone H3 deacetylation in cell homogenates of C2C12 cells, but neither

JPET Fast Forward. Published on October 5, 2012 as DOI: 10.1124/jpet.112.198937
This article has not been copyedited and formatted. The final version may differ from this version.

glycosyl RSVs nor RSV promoted histone H3 deacetylation *in vitro* (data not shown).

Our experiments showed that 4'G-RSV may be a useful RSV prodrug. In natural plants, 3G-RSV is one of the predominant glycosyl RSVs found, unlike 4'G-RSV (Romero-Perez et al., 1999). However, *E. coli* cells expressing glucosyltransferase from *Phytolacca Americana* produce 4'G-RSV and 3G-RSV from RSV at a ratio of 10:3, and the conversion rate of RSV to glycosyl RSVs is almost 100% after 24 h of incubation (Ozaki et al., 2012). *Phytolacca Americana* plant cell cultures also yielded high 4'G-RSV levels. Unlike RSV, which is highly hydrophobic, 4'G-RSV is hydrophilic, and may be highly useful for medical use such as treatment of diabetes mellitus and muscular dystrophy.

Authorship Contributions.

Participated in research design: Horio, Kuno, Wakamiya, and Hamada.

Conducted experiments: Hosoda, Kuno, Hori, Ohtani, and Oohiro.

Performed data analysis: Kuno, Wakamiya, Hamada, and Horio.

Wrote the manuscript: Horio, Kuno, and Hosoda.

References

Baur JA, et al. (2006) Resveratrol improves health and survival of mice on a high-calorie diet. *Nature* 444:337-342.

Boot RG, et al. (2007) Identification of the non-lysosomal glucosylceramidase as beta-glucosidase 2. *J Biol Chem* 282:1305-1312.

Chen Q, et al. (2010) Resveratrol induces growth arrest and apoptosis through activation of FOXO transcription factors in prostate cancer cells. *PLoS One* 5:e15288.

de Graaf M, et al. (2001) Cloning and characterization of human liver cytosolic beta-glycosidase. *Biochem J* 356:907-910.

Fabris S, Momo F, Ravagnan G and Stevanato R (2008) Antioxidant properties of resveratrol and piceid on lipid peroxidation in micelles and monolamellar liposomes. *Biophys Chem* 135:76-83.

Henry C, et al. (2005) Cellular uptake and efflux of trans-piceid and its aglycone trans-resveratrol on the apical membrane of human intestinal Caco-2 cells. *J Agric Food Chem* 53:798-803.

Hori YS, et al. (2011) Resveratrol ameliorates muscular pathology in the dystrophic mdx mouse, a model for Duchenne muscular dystrophy. *J Pharmacol Exp Ther* 338:784-794.

Horio Y, Hayashi T, Kuno A and Kunimoto R (2011) Cellular and molecular effects of sirtuins in health and disease. *Clin Sci* 121:191-203.

Howitz KT, et al. (2003) Small molecule activators of sirtuins extend Saccharomyces cerevisiae lifespan. *Nature* 425:191-196.

Jang M, et al. (1997) Cancer chemopreventive activity of resveratrol, a natural product derived from grapes. *Science* 275:218-220.

Juan ME, Gonzalez-Pons E and Planas JM (2010) Multidrug resistance proteins restrain the intestinal absorption of trans-resveratrol in rats. *J Nutr* 140:489-495.

Kacher Y, et al. (2008) Acid beta-glucosidase: insights from structural analysis and relevance to Gaucher disease therapy. *Biol Chem* 389:1361-1369.

Krasnow MN and Murphy TM (2004) Polyphenol glucosylating activity in cell suspensions of grape (Vitis vinifera). *J Agric Food Chem* 52:3467-3472.

Lagouge M, et al. (2006) Resveratrol improves mitochondrial function and protects against metabolic disease by activating SIRT1 and PGC-1alpha. *Cell* 127:1109-1122.

Mantei N, et al. (1988) Complete primary structure of human and rabbit lactase-phlorizin hydrolase: implications for biosynthesis, membrane anchoring and evolution of the enzyme. *Embo J* 7:2705-2713.

Matern H, Boermans H, Lottspeich F and Matern S (2001) Molecular cloning and

expression of human bile acid beta-glucosidase. *J Biol Chem* 276:37929-37933.

Morales FJ and Jimenez-Perez S (2001) Free radical scavenging capacity of Maillard reaction products as related to colour and fluorescence. *Food Chemistry* 72:119-125.

Ou B, Hampsch-Woodill M and Prior RL (2001) Development and validation of an improved oxygen radical absorbance capacity assay using fluorescein as the fluorescent probe. *J Agric Food Chem* 49:4619-4626.

Ozaki S, et al. (2012) Regioselective glucosidation of trans-resveratrol in Escherichia coli expressing glucosyltransferase from Phytolacca americana. *Biotechnol Lett* 34:475-481.

Prior, R. L.; Hoang, H.; Gu, L.; Wu, X.; Bacchiocca, M.; Howard, L.; Hampsch-Woodill, M.; Huang, D.; Ou, B.; Jacob, R. Assays for hydrophilic and lipophilic antioxidant capacity (oxygen radical absorbance capacity (ORACFL)) of plasma and other biological and food samples. J. Agric. Food Chem. 2003, 51, 3273-3279.

Regev-Shoshani G, Shoseyov O, Bilkis I and Kerem Z (2003) Glycosylation of resveratrol protects it from enzymic oxidation. *Biochem J* 374:157-163.

Romero-Perez AI, Ibern-Gomez M, Lamuela-Raventos RM and de La Torre-Boronat MC (1999) Piceid, the major resveratrol derivative in grape juices. *J Agric Food Chem* 47:1533-1536.

Sakamoto J, Miura T, Shimamoto K and Horio Y (2004) Predominant expression of Sir2alpha, an NAD-dependent histone deacetylase, in the embryonic mouse heart and brain. *FEBS Lett* 556:281-286.

Su HC, Hung LM and Chen JK (2006) Resveratrol, a red wine antioxidant, possesses an insulin-like effect in streptozotocin-induced diabetic rats. *Am J Physiol Endocrinol Metab* 290:E1339-1346.

Sun AY, Wang Q, Simonyi A and Sun GY (2010) Resveratrol as a therapeutic agent for neurodegenerative diseases. *Mol Neurobiol* 41:375-383.

Tanno M, et al. (2010) Induction of manganese superoxide dismutase by nuclear translocation and activation of SIRT1 promotes cell survival in chronic heart failure. *J Biol Chem* 285:8375-8382.

Vogt T and Jones P (2000) Glycosyltransferases in plant natural product synthesis: characterization of a supergene family. *Trends Plant Sci* 5:380-386.

Wang X, et al. (2012) Polydatin, a natural polyphenol, protects arterial smooth muscle cells against mitochondrial dysfunction and lysosomal destabilization following hemorrhagic shock. *Am J Physiol Regul Integr Comp Physiol* 302:R805-814.

Weis M, Lim EK, Bruce N and Bowles D (2006) Regioselective glucosylation of aromatic compounds: screening of a recombinant glycosyltransferase library to identify

biocatalysts. Angew Chem Int Ed Engl 45:3534-3538.

Wright EM, Loo DD and Hirayama BA (2011) Biology of human sodium glucose transporters. *Physiol Rev* 91:733-794.

Wu JM and Hsieh TC (2011) Resveratrol: a cardioprotective substance. *Ann N Y Acad Sci* 1215:16-21.

Yang NC, Lee CH and Song TY (2010) Evaluation of resveratrol oxidation in vitro and the crucial role of bicarbonate ions. *Biosci Biotechnol Biochem* 74:63-68.

Footnotes

This work was supported by the Ministry of Education, Culture, Sports, Science, and Technology of Japan [Grant-in-Aid 22590245]; by a National Project of the Knowledge Cluster Initiative (Second Stage); by Sapporo Biocluster Bio-S; by the Program for Developing the Supporting System for Upgrading Education and Research; and by the Regional R&D Proposal-Based Program from the Northern Advancement Center for Science & Technology of Hokkaido Japan.

Figure legends

Fig. 1. RSV and glycosyl RSV *in vitro* antioxidant activity. (A) Chemical structures of resveratrol (RSV), resveratrol 3-O-β-D-glucoside (3G-RSV), and resveratrol 4'-O-β-D-glucoside (4'G-RSV). (B) The DPPH radical-scavenging activity of RSV, 3G-RSV, and 4'G-RSV.

Fig. 2. RSV and 4'G-RSV promote histone H3 deacetylation and induce SOD2. (A) Representative immunoblots and amounts of acetyl histone H3 (AcH3) and total histone H3 (Total H3) in C2C12 cells treated with vehicle (control) or 100 μM resveratrol (RSV), resveratrol 3-O-β-D-glucoside (3G-RSV), or resveratrol 4'-O-β-D-glucoside (4'G-RSV) for 24 h. Data were analyzed from 3 independent experiments. (B-D) Cells were treated with vehicle (control) or 100 μM RSV, 3G-RSV, or 4'G-RSV for 24 h; 100 μM antimycin A was added 6 h before harvest to induce oxidative stress. (B) SOD2 mRNA levels from three independent experiments. (C) Representative SOD2 immunostaining and nuclear staining images in C2C12 cells, and quantitative analysis from six independent experiments. Red and blue indicate SOD2 staining and nuclei, respectively. (D) Representative immunoblots of SOD2 and GAPDH, and their levels measured in C2C12 cells in 6 independent experiments. Bars indicate S.E.M.; n.s., not

significant.

Fig. 3. SIRT1-dependent histone H3 deacetylation and SOD2 induction by RSV and 4'G-RSV. (A) Representative immunoblots for SIRT1 and α-tubulin, and SIRT1 protein levels in C2C12 cells transfected with control-siRNA or SIRT1-siRNA (n = 6). (B) Representative immunoblots and amounts of acetyl histone H3 (AcH3) and total histone H3 (Total H3). C2C12 cells were transfected with control-siRNA or SIRT1-siRNA, and then treated with vehicle (control) or 100 μM RSV, 3G-RSV, or 4'G-RSV for 12 h. Data are from seven independent experiments. (C) Representative SOD2 and α-tubulin immunoblots. C2C12 cells were transfected with control- or SIRT1-siRNA and then treated with vehicle (control) or 100 μM RSV, 3G-RSV, or 4'G-RSV for 24 h; 100 μM antimycin A (AA) was added 6 h before harvest to induce oxidative stress. Data from six independent experiments were compared. Bars indicate S.E.M.; n.s., not significant.

Fig. 4. RSV and 4'G-RSV inhibit oxidative stress-induced apoptosis in C2C12 cells and neonatal rat cardiomyocytes. (A, B) C2C12 cells were treated with

JPET Fast Forward. Published on October 5, 2012 as DOI: 10.1124/jpet.112.198937
This article has not been copyedited and formatted. The final version may differ from this version.

vehicle (control) or 30 μM RSV, 3G-RSV, or 4'G-RSV for 12 h. AA (50 μM) was added 8 h before fixation to induce apoptosis. (A) Representative images of apoptotic C2C12 cells showing nuclear condensation (arrows). Cells were stained with Hoechst 33342 (blue). The percentage of cells with condensed nuclei is shown (right panel); cells were counted in four independent experiments. Bars indicate S.E.M.; n.s., not significant. (B) Representative images of activated caspase-3. AA-treated C2C12 cells were stained with anti-activated caspase-3 antibody (green) and Hoechst 33342 (red). Nuclei are shown by red as a pseudocolor to identify activated caspase-3 staining in nuclei (yellow). Arrows indicate activated caspase-3^+ apoptotic cells. The percentage of apoptotic cells is shown in the right panel; cells were counted in four independent experiments. Bars indicate S.E.M.; n.s., not significant. (C) Representative images of TUNEL staining (green), propidium iodide (PI) staining (red), and nuclei (blue) in neonatal rat ventricular myocytes. Isolated cardiomyocytes were stained with PI to identify dead cells before pharmacological modulation, and PI^+ cells were eliminated from statistical analysis. Cells were treated with vehicle (control) or 40 μM RSV, 3G-RSV, or 4'G-RSV for 36 h. AA (100 μM) was added 24 h before harvest to induce

apoptosis. TUNEL-positive cells are indicated by arrows. Right panel shows percentages of TUNEL-positive cells. Data from six independent experiments were compared.

Fig. 5. RSV and 4'G-RSV inhibit cell proliferation in C2C12 cells. Representative images (upper panels) of C2C12 cells treated with vehicle (control) or 30 μM RSV, 3G-RSV, or 4'G-RSV for 24 h. Nuclei were stained by Hoechst 33342. Cell counts were from six independent experiments. Bars indicate S.E.M.; n.s., not significant.

Fig. 6. ESI-MS analyses of cell extracts treated with RSV or glycosyl RSVs. ESI-MS spectra of intracellular fractions from C2C12 cells treated with 100 μM RSV (A), 3G-RSV (B), or 4'G-RSV (C) for 12 h. Cells were washed with PBS twice, lysed, extracted with methanol, and analyzed by ESI-MS. Arrows and arrowheads indicate the position of RSV and glycosyl RSVs, respectively.

Fig. 7. HPLC analyses of culture medium and cell extracts treated with RSV or glycosyl RSVs. C2C12 cells were treated with 100 μM RSV, 3G-RSV, or

JPET Fast Forward. Published on October 5, 2012 as DOI: 10.1124/jpet.112.198937
This article has not been copyedited and formatted. The final version may differ from this version.

4’G-RSV for 12 h, washed with PBS twice, and lysed. Samples were extracted from culture medium or cell lysates with methanol and were analyzed by HPLC. HPLC profiles of extracts from (A) extracellular fractions (culture medium) and (B) intracellular fractions from C2C12 cells incubated with RSV (upper panels), 3G-RSV (middle panels), or 4’G-RSV (lower panels). RSV and glycosyl RSVs were monitored by absorbance at 323 nm.

TABLE1

ORAC values

	mmolTE/mg	mmolTE/mmol
RSV	33.1	7.6
3G-RSV	24.6	9.6
4'G-RSV	8.0	3.1

The ORAC value was expressed as micromoles of Trolox equivalent (TE) per micromole of sample. RSV, resveratrol; 3G-RSV, resveratrol 3-O-β-D-glucoside; 4'G-RSV, resveratrol 4'-O-β-D-glucoside.

JPET Fast Forward. Published on October 5, 2012 as DOI: 10.1124/jpet.112.198937
This article has not been copyedited and formatted. The final version may differ from this version.

TABLE2

Extracellular and Intracellular amounts of RSV and glycosyl RSVs

		Extracellular fraction			Intracellular fraction		
		RSV	3G-RSV	4'G-RSV	RSV	3G-RSV	4'G-RSV
Treatment	RSV	17.04 ± 1.20	n.d	n.d	5.34 ± 0.14	n.d	n.d
	3G-RSV	n.d	15.99 ± 0.31	n.d	n.d	n.d	n.d
	4'G-RSV	32.33 ± 0.51	n.d	4.44 ± 0.57	2.34 ± 0.22	n.d	n.d

C2C12 cells in a 10-cm dish were incubated with 100 μM RSV, 3G-RSV, or 4’G-RSV for 12 h, after which RSV or glycosyl RSVs were extracted from culture medium (Extracellular fraction) and cell pellets (Intracellular fraction) and were separated by HPLC. Values were shown by means ± S.E.M. (nmoles). n=3. RSV, resveratrol; 3G-RSV, resveratrol 3-O-β-D-glucoside; 4'G-RSV, resveratrol 4'-O-β-D-glucoside; n.d, not detected.

JPET Fast Forward. Published on October 5, 2012 as DOI: 10.1124/jpet.112.198937

Figure 1

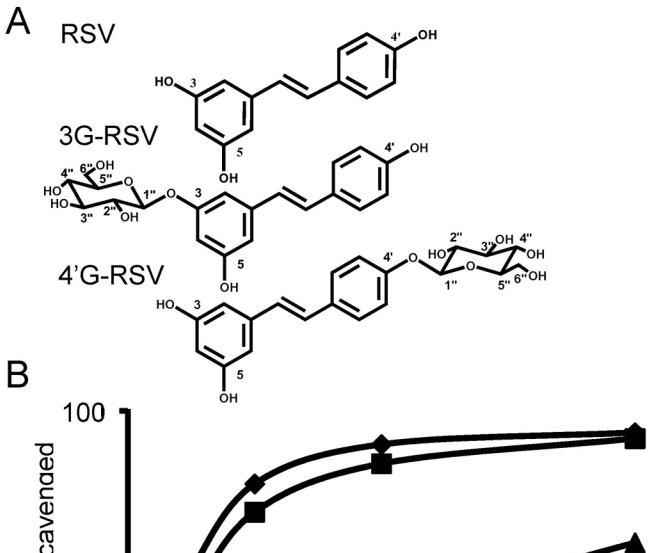

Figure 2

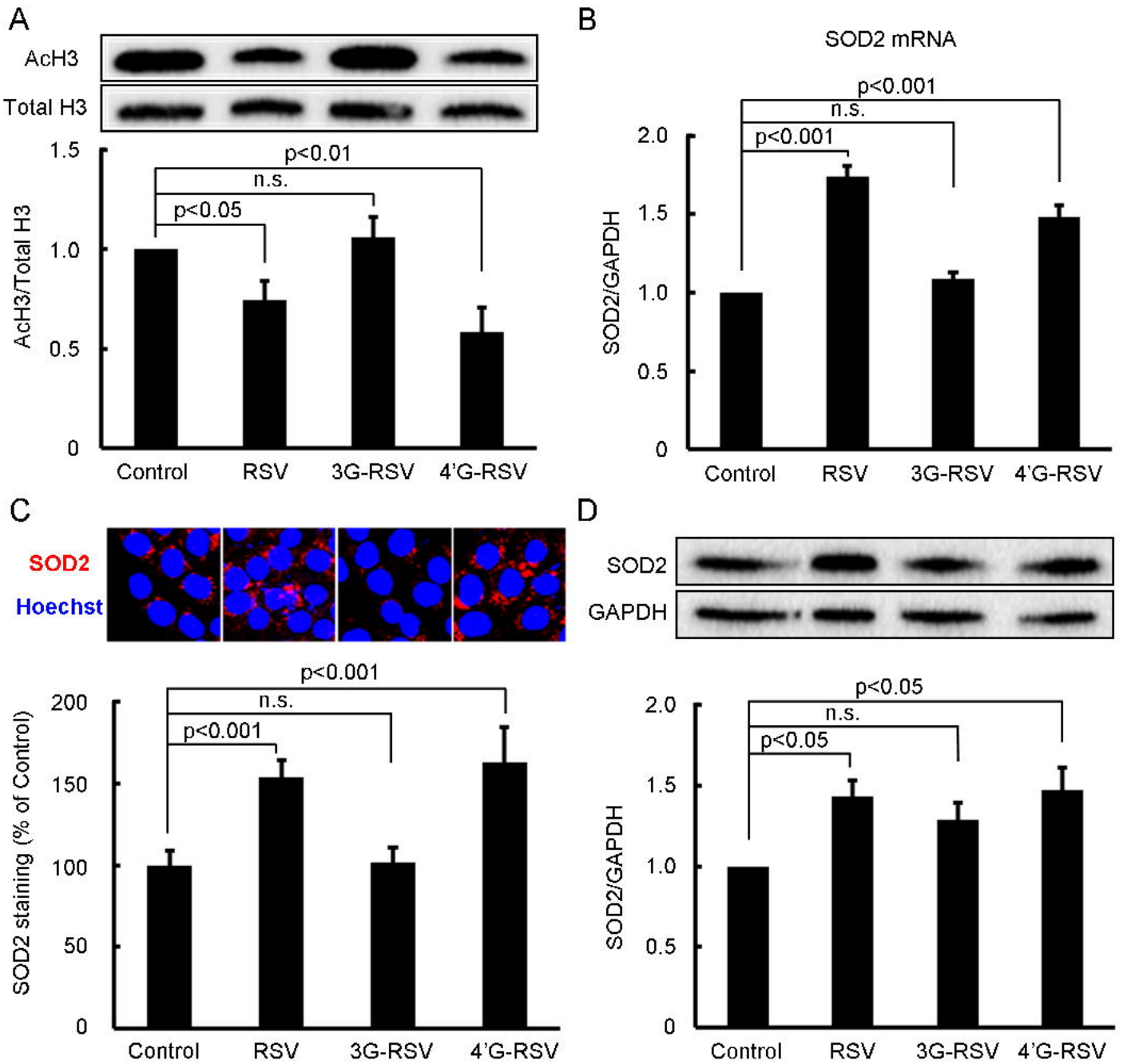
A
AcH3
Total H3
AcH3/Total H3
p<0.01
n.s.
p<0.05
Control
RSV
3G-RSV
4'G-RSV
B
SOD2 mRNA
p<0.001
n.s.
p<0.001
SOD2/GAPDH
C
SOD2
Hoechst
p<0.001
n.s.
p<0.001
SOD2 staining (% of Control)
D
SOD2
GAPDH
p<0.05
n.s.
p<0.05
SOD2/GAPDH

JPET Fast Forward. Published on October 5, 2012 as DOI: 10.1124/jpet.112.198937
This article has not been copyedited and formatted. The final version may differ from this version.

Figure 3

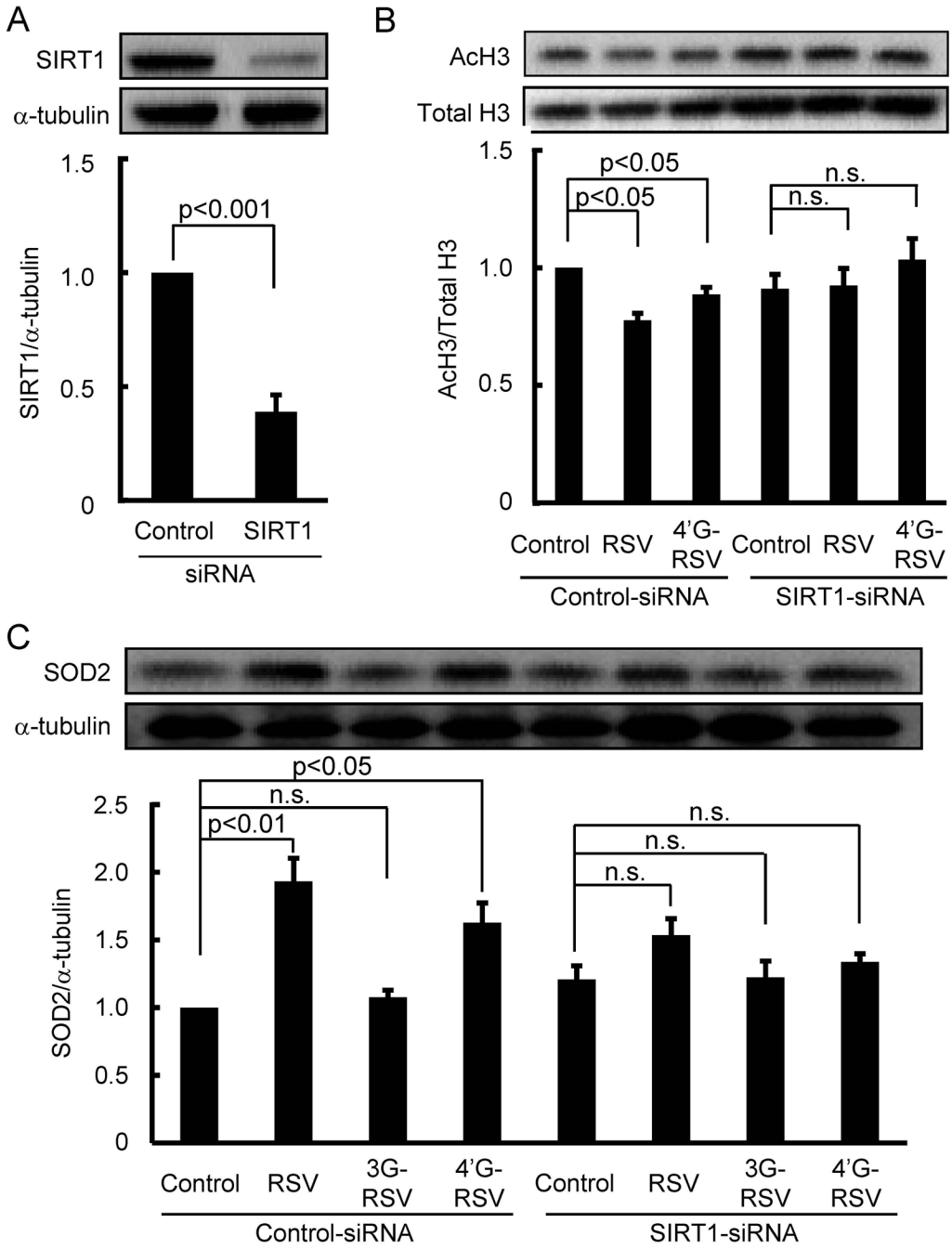

Figure 4

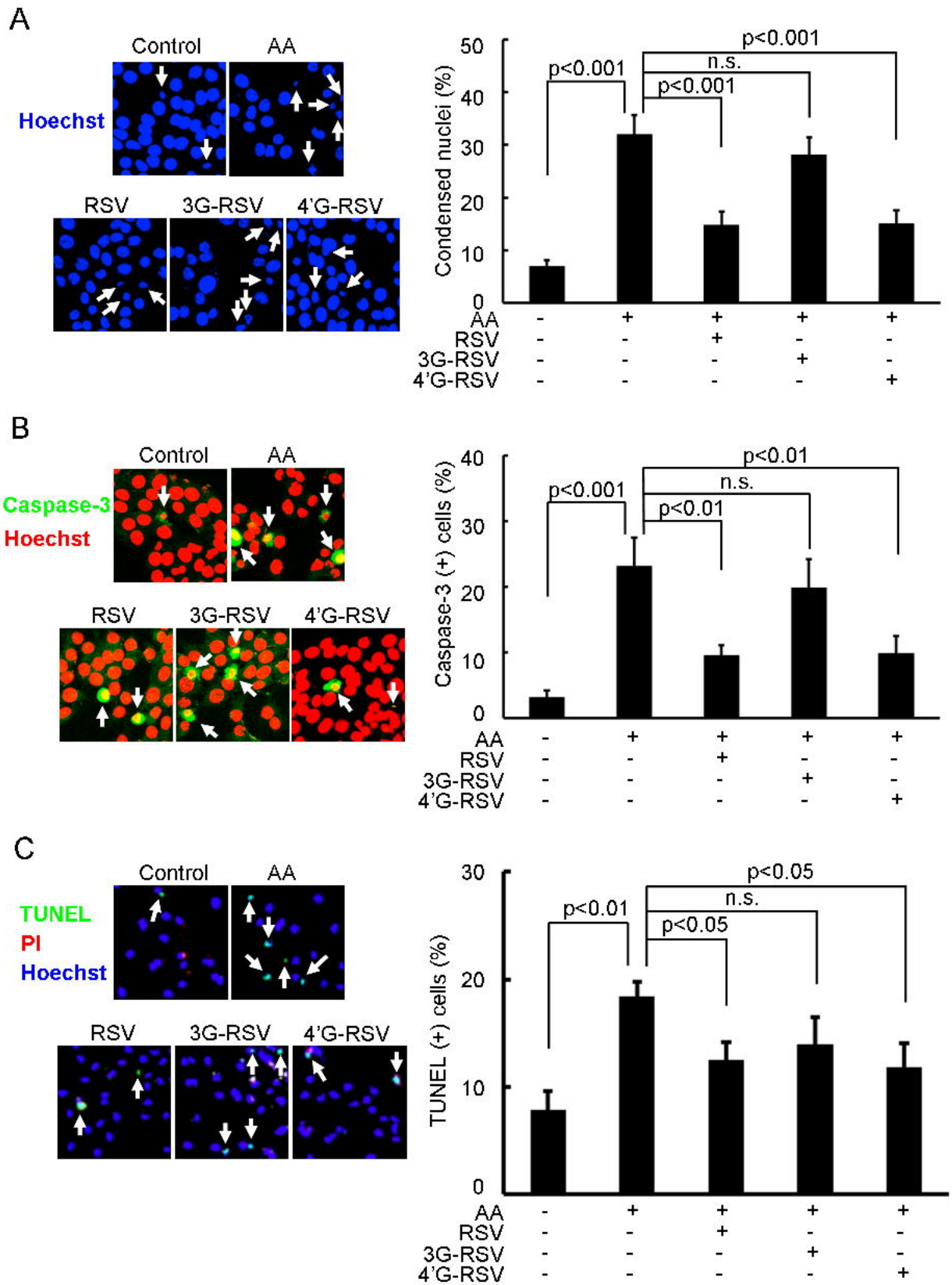
A
Control
AA
Hoechst
RSV
3G-RSV
4'G-RSV
Condensed nuclei (%)
p<0.001
p<0.001
n.s.
p<0.001
AA
RSV
3G-RSV
4'G-RSV
B
Caspase-3
Hoechst
Caspase-3 (+) cells (%)
p<0.001
p<0.01
n.s.
p<0.01
C
TUNEL
PI
Hoechst
TUNEL (+) cells (%)
p<0.01
p<0.05
n.s.
p<0.05

JPET Fast Forward. Published on October 5, 2012 as DOI: 10.1124/jpet.112.198937
This article has not been copyedited and formatted. The final version may differ from this version.

Figure 5

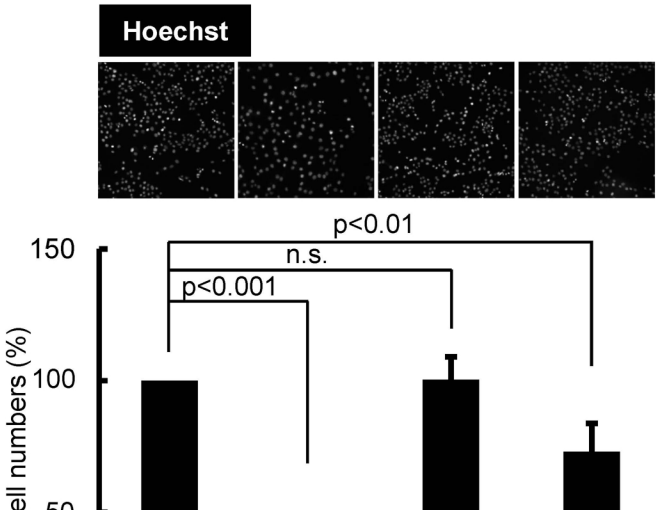

Figure 6

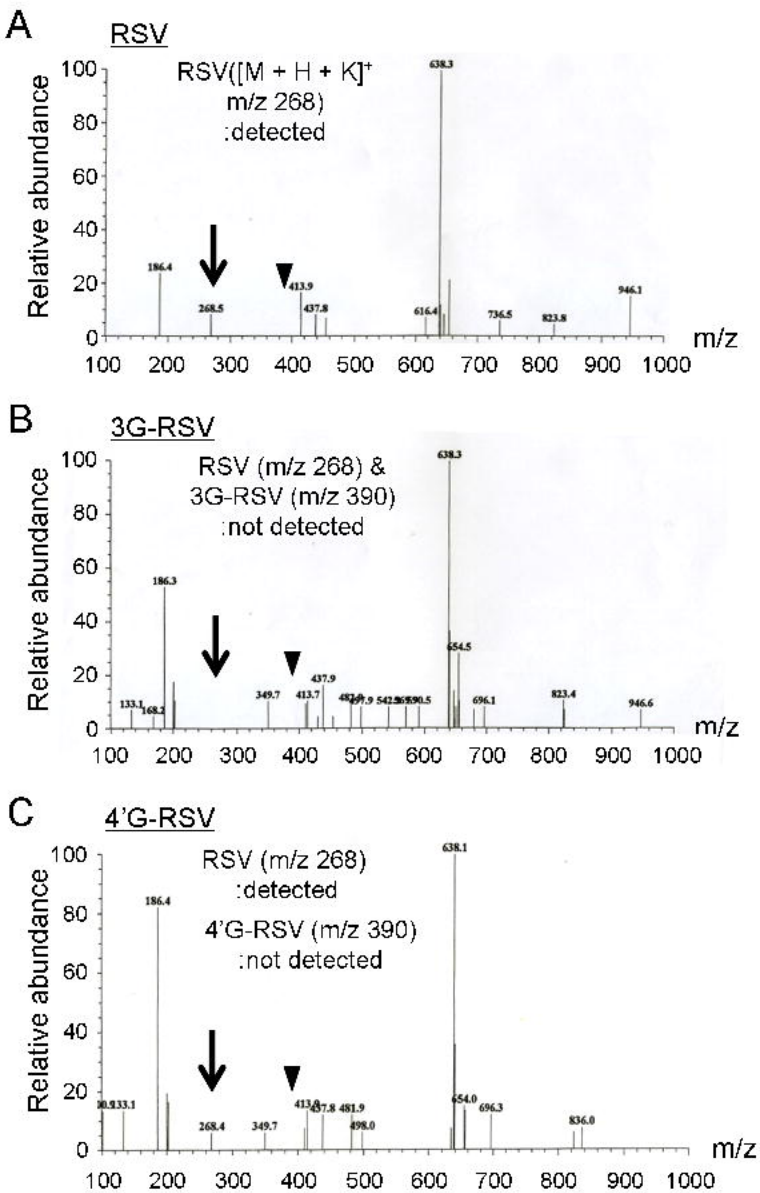
A
RSV
RSV([M + H + K]+ m/z 268) :detected
Relative abundance
m/z
B
3G-RSV
RSV (m/z 268) & 3G-RSV (m/z 390) :not detected
Relative abundance
m/z
C
4'G-RSV
RSV (m/z 268) :detected
4'G-RSV (m/z 390) :not detected
Relative abundance
m/z

Figure 7

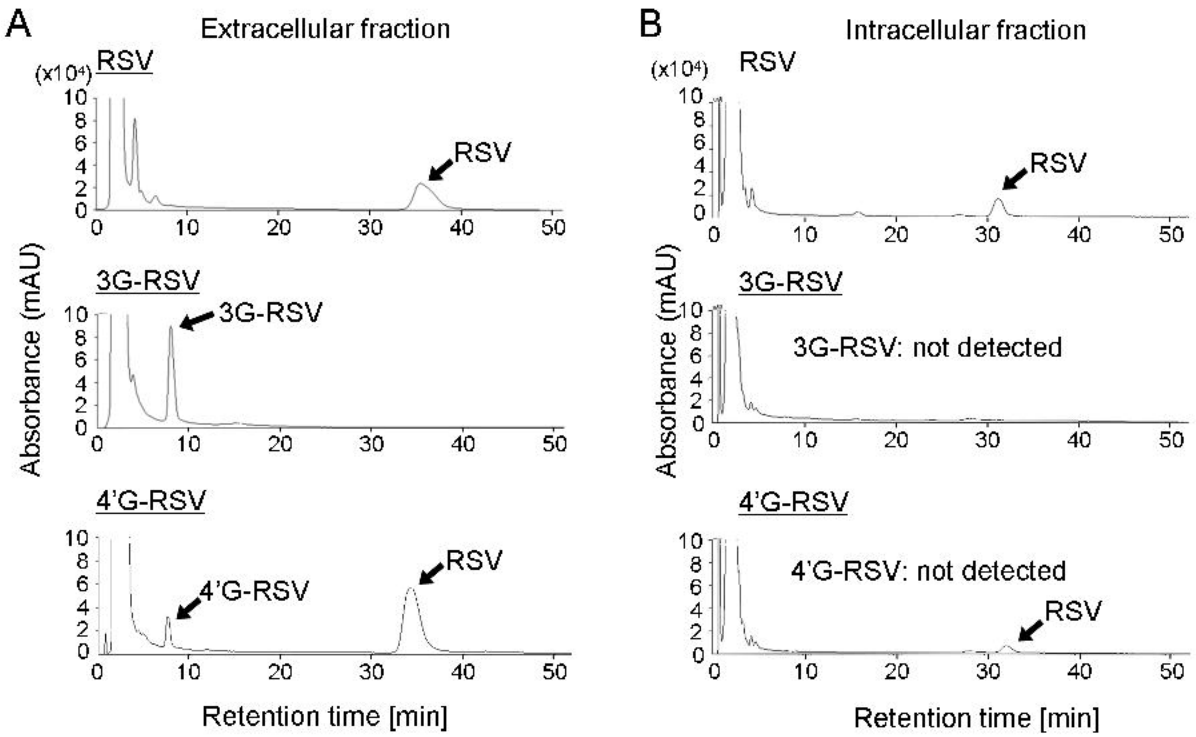
A
Extracellular fraction
(x10⁴)
RSV
RSV
3G-RSV
3G-RSV
4'G-RSV
4'G-RSV
RSV
Absorbance (mAU)
Retention time [min]
B
Intracellular fraction
(x10⁴)
RSV
RSV
3G-RSV
3G-RSV: not detected
4'G-RSV
4'G-RSV: not detected
RSV
Absorbance (mAU)
Retention time [min]